International Journal of Biology and Life Sciences
ISSN: 2957-9511 | Vol. 5, No. 3, 2024

The Feasibility Study of Carotid Artery Stent Implantation Surgery Simulation based on CFD Technology

Yanhan Song [3], Xue Wang [1], Yikai Meng [2], Xin Lin [1], Xinyue Zhang [2], Xinyu Liang [3], Na Zhu [4], Hongfei Zhu [4], Guo Yu [3], Wendi Sun [3], Liya Wang [2], Jianhui Wu [1, *]

[1] School of Public Health, North China University of Science and Technology, Tangshan Hebei, 063210, China
[2] College of Science, North China University of Science and Technology, Tangshan Hebei, 063009, China
[3] Traditional Chinese Medicine College, North China University of Science and Technology, Tangshan Hebei, 063210, China
[4] Clinical Medical College, North China University of Science and Technology, Tangshan Hebei, 063000, China

*** Corresponding author:** Jianhui Wu

Abstract: Carotid artery stenting (CAS) is an emerging endovascular intervention technique that has the potential to reduce the risk of stroke; however, it may be associated with a variety of complications postoperatively. Consequently, it is imperative to identify risk factors prior to CAS preoperative. Computational Fluid Dynamics (CFD) simulation uses numerical calculation methods to simulate and analyze the physical phenomena of blood flow. This research leverages a carotid ultrasound database to construct 3D models and conducts stent implantation simulations at sites of carotid stenosis to predict postoperative recovery outcomes. By providing more comprehensive and accurate information as feasibly as possible, the aim is to assist physicians in optimizing surgical plans, enhancing the success rate of surgeries, minimizing operative risks and ultimately delivering superior therapeutic results to patients.

Keywords: Carotid Artery Stenting; 3D Blood Vessel Model; CFD Simulation.

1. Introduction

Stroke, also known as ischemic stroke (IS) [1], is a type of cerebrovascular disease characterized by sudden onset and rapid changes, resulting from cerebral ischemia caused by vascular occlusion or rupture, leading to damage to brain tissue. Ischemic stroke accounts for approximately 70% of all stroke cases, with carotid artery stenosis contributing to 15% to 20% of ischemic stroke etiology [2] [3]. Therefore, investigating the occurrence, progression, and factors influencing plaque rupture in carotid artery stenosis is crucial for the clinical management and prevention of ischemic stroke.

At present, the gold standard method for clinically diagnosing carotid atherosclerotic plaques is CT angiography. While this method boasts high accuracy, its invasive nature poses potential trauma risks, and some patients may exhibit allergic reactions to contrast agents, rendering it unsuitable for certain diagnostic purposes. Ultrasound, on the other hand, is a commonly used non-invasive technique for diagnosing diseases such as carotid artery stenosis and is frequently employed in screening for carotid artery stenosis. Therefore, there is a clinical need to find a safer, equally accurate, and more widely available method for diagnosing carotid atherosclerotic plaques. Ultrasound, being safe, non-invasive, not requiring contrast agents, and relatively inexpensive, is one of the preferred diagnostic methods for patients with carotid atherosclerotic plaques.

In recent years, propelled by the advancements in computer technology, computational fluid dynamics (CFD) has swiftly risen as a cornerstone tool in hemodynamics research. This approach entails simulating and scrutinizing fluid movement patterns, converting them into mathematical equations to procure intricate insights into fluid motion. in cardiovascular research, CFD-based numerical simulations not only allow for the analysis of conventional fluid parameters like flow direction and velocity but also enable the assessment of intricate flow patterns and stress distributions. Additionally, they provide parameters that traditional imaging techniques cannot measure, such as wall shear stress.

This study is grounded in carotid artery stenosis ultrasound images to develop three-dimensional models both pre and post carotid artery stent implantation. Through the observation of hemodynamic alterations, the study seeks to accomplish a preoperative evaluation of carotid artery stenting (CAS) treatment for carotid artery stenosis, thereby offering valuable clinical insights.

2. Material and Methods

2.1. General Information

The image data was obtained from an 83-year-old female patient who was scheduled to undergo internal carotid artery stenting (CAS) due to carotid artery stenosis. A linear array probe with a frequency of 7-10 MHz was selected, and 72 ultrasound images of the head and neck before and after CAS were continuously collected with the German Siemens S2000 color Doppler ultrasound diagnostic instrument.

2.2. Research Methods

(1) Lesion environment modeling and implantation simulation

In the current investigation, mimics, Geomagic and solid works software were used to construct the vascular models before and after CAS. Firstly, the 3D data and images of the patients' common carotid artery, internal carotid artery and external carotid artery collected by Doppler color ultrasound were used to reconstruct the original carotid artery stenosis model in mimics, and the point cloud format model was obtained; Then, Geomagic software is used to repair and transform the model to build the solid model [4]; Finally, the solid works software [5] was used for editing and modification, and the solid model of the implanted stent was constructed and placed in the modified lesion to simulate CAS. The length of the stent model was set to cover the carotid artery stenosis, and both ends of the stent model exceeded the stenosis area, and the diameter was slightly larger than the normal diameter of the carotid artery, as shown in Figure 1.

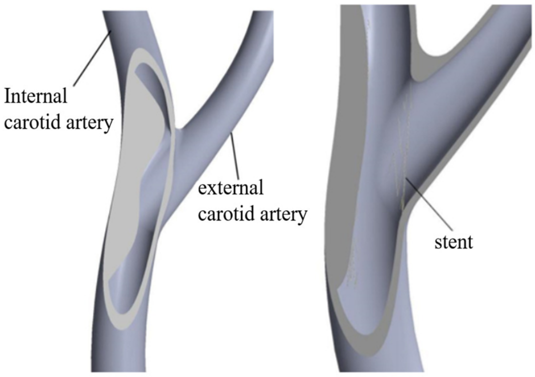

Figure 1. Cross-section models of vessels before and after CAS

(2) Hemodynamic analysis

Firstly, the ANSYS FLUENT software was used to divide the grid of the carotid artery blood fluid area, and then the setting module was entered to set the model materials. Blood was set as incompressible Newtonian fluid, and the blood density was set as 1050 kg/m3, the viscosity was set as 0.0035 kg/m-s, the carotid artery vessel wall was set as rigid wall, no slip, and no permeability. the inlet velocity was set as 1.4 m/s, and the outlet pressure was set as 0 pa. The carotid artery wall thickness was large but equivalent to the small diameter of the carotid artery, so the influence of wall thickness on flow field distribution could be ignored. Therefore, for blood flow analysis, we adopted the standard k-epsilon turbulence formula and the standard wall function (SWF)[6].

3. Results

3.1. Ultrasound Images of the Head and Neck

Figure 2(A) shows the preoperative examination image of the patient. According to the examination report, the lumen structure of the bilateral common carotid artery, internal carotid artery and external carotid artery was clear, and the intima was not smooth. Multiple plaques were found in the right carotid artery. The large one was located at the posterior wall of the common carotid artery bifurcation extending to the beginning of the internal carotid artery, which was a mixed echo plaque with a size of about 0.3×1.4 cm. The initial lumen stenosis rate of the internal carotid artery was about 52%. Multiple plaques were found in the left carotid artery. The large one was located at the posterior wall of the common carotid artery bifurcation, which was a mixed echo plaque with a size of about 0.31×1.3 cm, resulting in stenosis of the common carotid artery bifurcation lumen, and the diameter stenosis rate was about 38%.

Figure 2(B) is the postoperative examination image of the patient. This examination found that after the right carotid artery stent implantation, the strong echo of the stent could be seen in the segment from the right common carotid artery to the beginning of the internal carotid artery, and the blood flow in the stent was unblocked. The proximal end of the stent was 0.43 cm, the distal end was 0.39cm, the smallest part of the stent was in the middle segment, and the blood flow bundle was about 0.24 cm. Multiple plaques were found in the right carotid artery, the largest located between the stent and the arterial wall[7].

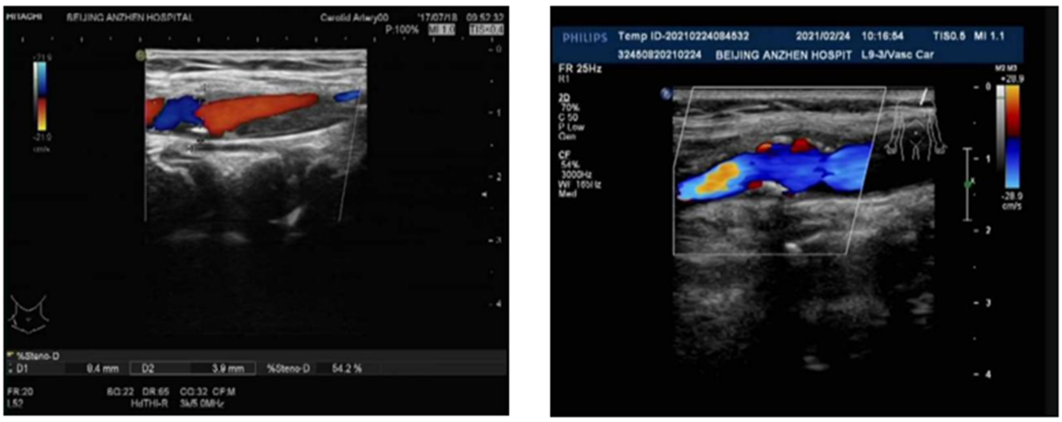

(A) (B)

Figure 2. Ultrasound images of the head and neck. (A) Preoperative SONographic FINDINGS. (B) Simulated postoperative SONographic FINDINGS

3.2. Velocity Flow Diagram

velocity maps can reflect the flow and distribution of blood. Peak systolic velocity (PSV) refers to the maximum blood flow velocity of blood vessels examined by ultrasound during cardiac contraction. Before CAS, as shown in Figure 3(A), the blood flow velocity of the right common carotid artery and the internal carotid artery stenosis was higher, with PSV of about 187 cm/s. The blood flow velocity of the internal carotid artery was higher than that of the external carotid artery, with PSV of about 236 cm/s[8].

After the initial stenting of the right common carotid artery extended to the internal carotid artery, the blood flow in the stent was unobstructed, as shown in Figure 3(B). The blood flow velocity at the stent placement was lower than that at other stenosis sites, PSV=86 cm/s, and PSV=156 cm/s at the distal segment, that is, the internal carotid artery. Multiple plaques were found in the right carotid artery, and the largest plaque was located at the posterior wall of the common carotid artery bifurcation extending to the beginning of the internal carotid artery. The multiple plaques caused luminal stenosis at the right common carotid artery bifurcation, and the PSV at the stenosis was 126 cm/s.

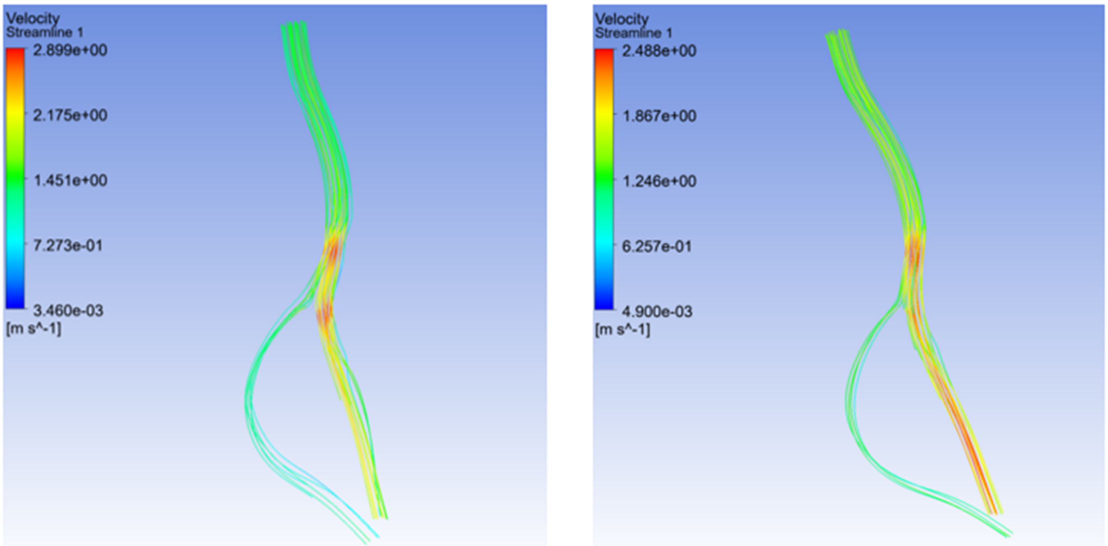

(A) **(B)**

Figure 3. Velocity flow diagram. (A) Velocity-flow diagram before CAS. (B) Velocity-flow diagram after CAS

3.3. Wall Pressure Diagram

Before CAS, as shown in Figure 4(A), the wall pressure of the common carotid artery bifurcation extending to the internal carotid artery and the external carotid artery was relatively high, especially the pressure of the common carotid artery and the anterior part of the plaque where the bifurcation extended to the beginning of the internal carotid artery was relatively high, and the pressure distribution was uneven.

After the operation, the pressure of the upper segment of the common carotid artery was still high, but the pressure gradually decreased as the blood flowed into the bifurcation. On the two branches, the pressure of the internal carotid artery was slightly higher than that of the external carotid artery, and an obvious area of high pressure appeared at the bifurcation apex, as shown in Figure 4(B).

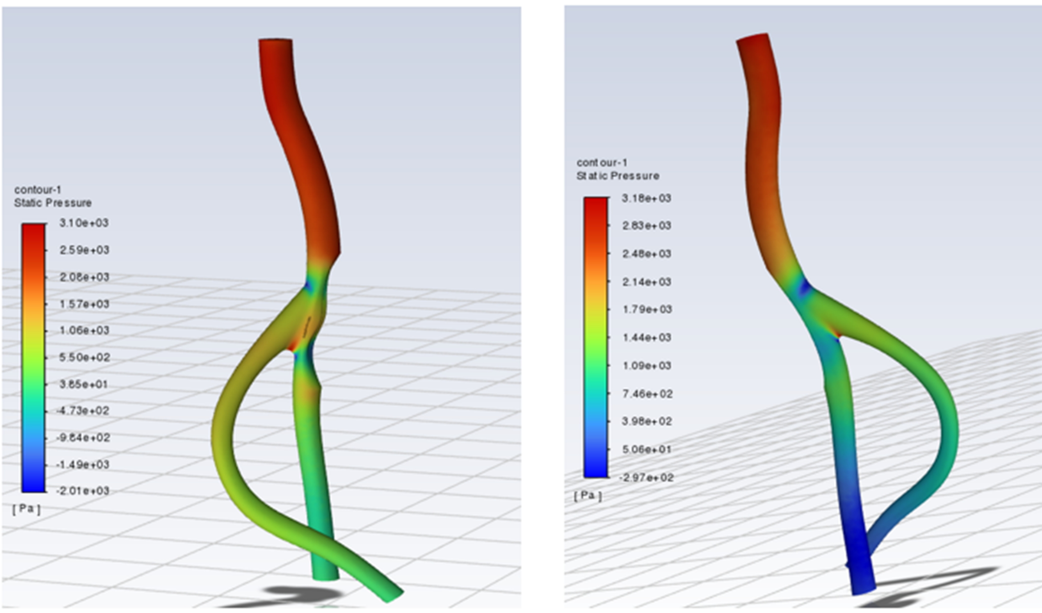

(A) **(B)**

Figure 4. Wall pressure diagram. (A) Wall pressure diagram before CAS. (B) Wall pressure diagram after CAS

4. Discussion

Using CFD allows obtaining hemodynamic parameters that are difficult to measure directly in clinical practice, quantitatively assessing blood perfusion after CAS treatment for carotid artery stenosis, which helps predict the effectiveness of CAS[9].Our study extensively researched carotid artery stenosis using 3D reconstruction technology. The narrowing was processed and reverse reconstructed using Mimics, Geomagic, and Solidworks software. The 3D model was manually manipulated to create a stenosis removal treatment model, followed by finite element analysis. Through this personalized numerical simulation method, doctors can gain a more precise understanding of the blood flow inside the patient's blood vessels, aiding in the development of more customized treatment plans[10][11].

Research has also found that stent placement directly alters the blood flow environment within the blood vessels, and hemodynamic factors are closely related to vascular remodeling. Abnormal blood flow can lead to changes in hemodynamic factors, thereby triggering vascular remodeling diseases. For moderate stenosis of the carotid artery, de-stenosis treatment can improve blood flow perfusion, but the impact is not significant and the treatment method need to be selected according to the specific situation of the patient.

In summary, this study introduces a method for simulating CA, which can assist doctors in diagnosing and treating patients with unclear surgical indications.

This study has the following limitations: due to individual differences and the complexity of surgical procedures, there may be discrepancies between the simulation results and actual situations; furthermore, simulating the behavior of stent materials requires consideration of material nonlinearity, fatigue, and damage characteristics, which increases the difficulty of the simulation. Future follow-up studies will increase the sample size and track the analysis and comparison of actual postoperative case data of patients to improve the accuracy and reliability of the method.

Acknowledgments

Supported by National undergraduate innovation and entrepreneurship training program of China (202310081007);

2023 North China University of Science and Technology Undergraduate Innovation and Entrepreneurship Training Program Project (R2023036).

References

[1] Li, L. D., Zhou, Y., & Shi, S. F. (2024). Identification and characterization of biomarkers associated with endoplasmic reticulum protein processing in cerebral ischemia-reperfusion injury. PeerJ, 12, e16707.

[2] GBD 2019 Stroke Collaborators (2021). Global, regional, and national burden of stroke and its risk factors, 1990-2019: a systematic analysis for the Global Burden of Disease Study 2019. The Lancet. Neurology, 20(10), 795–820.

[3] Tsao, C. W., Aday, A. W., Almarzooq, Z. I., Alonso, A., Beaton, A. Z., Bittencourt, M. S., Boehme, A. K., Buxton, A. E., Carson, A. P., Commodore-Mensah, Y., Elkind, M. S. V., Evenson, K. R., Eze-Nliam, C., Ferguson, J. F., Generoso, G., Ho, J. E., Kalani, R., Khan, S. S., Kissela, B. M., Knutson, K. L., … Martin, S. S. (2022). Heart Disease and Stroke Statistics-2022 Update: A Report from the American Heart Association. Circulation, 145(8), e153–e639.

[4] Curcio, N., Rosato, A., Mazzaccaro, D., Nano, G., Conti, M., & Matrone, G. (2023). 3D patient-specific modeling and structural finite element analysis of atherosclerotic carotid artery based on computed tomography angiography. Scientific reports, 13(1), 19911.

[5] Yan, X. T. (2011). Parameterized Modeling of Parts Based on SolidWorks. Advanced Materials Research, 346, 394–397.

[6] Bai-Nan, X., Fu-Yu, W., Lei, L., Xiao-Jun, Z., & Hai-Yue, J. (2011). Hemodynamics model of fluid-solid interaction in internal carotid artery aneurysms. Neurosurgical review, 34(1), 39–47.

[7] Pisu, F., Chen, H., Jiang, B., Zhu, G., Usai, M. V., Austermann, M., Shehada, Y., Johansson, E., Suri, J., Lanzino, G., Benson, J., Nardi, V., Lerman, A., Wintermark, M., & Saba, L. (2023). Machine learning detects symptomatic patients with carotid plaques based on 6-type calcium configuration classification on CT angiography. European radiology, 10.1007/s00330-023-10347-2. Advance online publication.

[8] H.N. Abhilash,Yoshiki Yanagita,Raghuvir Pai,Mohammad Zuber, Masaaki Tamagawa, Prakashini K... & S.M. Abdul Khader. (2024). Effect of vascular geometry on haemodynamic changes in a carotid artery bifurcation using numerical simulation. Clinical Neurology and Neurosurgery 108153-.

[9] Yao, X., Dai, Z., Zhang, X., Gao, J., Xu, G., Cai, Y., & Li, Z. (2019). Carotid Geometry as a Predictor of In-Stent Neointimal Hyperplasia- A Computational Fluid Dynamics Study. Circulation journal: official journal of the Japanese Circulation Society, 83(7), 1472–1479.

[10] Onal, Y., & Samanci, C. (2020). Is there any relationship between carotid bifurcation geometry and hemodynamic depression after carotid stenting and angioplasty?. International angiology: a journal of the International Union of Angiology, 39 (1), 17–23.

[11] Liu, H., Liu, Y., Ip, B. Y. M., Ma, S. H., Abrigo, J., Soo, Y. O. Y., Leung, T. W., & Leng, X. (2022). Effects of stent shape on focal hemodynamics in intracranial atherosclerotic stenosis: A simulation study with computational fluid dynamics modeling. Frontiers in neurology, 13, 1067566.